CHAPTER 4

STUDY OF BISTATIC SCATTERING RESPONSE OF WHEAT CROP FOR THE ESTIMATION OF CROP GROWTH PARAMETERS USING A FUZZY INFERENCE SYSTEM AT X-, C-, AND L-BANDS FOR CO-POLARIZATIONS

4.1 INTRODUCTION

Crops/vegetations monitoring at regular intervals is essential for the economic development of any nation. The importance of agricultural monitoring is to take appropriate measures and to assess information about probable losses in the production. The study of change in crop growth parameters at different crop growth stages is essential for monitoring and predicting the crop yield (Liakos et al. 2018). However, estimation of crop growth parameters based on field measurements are often expensive, prone to enormous errors and are unable to provide the real-time, spatially explicit information or forecasting of crops condition. The uses of remote sensing systems provide temporally, spatially, and repetitively monitoring of most of the globe. At the same time, the development of satellite remote sensing data has become the topmost data source to monitor crop conditions on a large-scale and regular basis. Remote sensing based on optical sensors have the most important limit is that their operational use are weather dependent, since visible/IR wavelengths are hampered by cloudy weather conditions. Therefore, at this juncture, another remote sensing technique is required which can overcome the above mentioned restriction in optical remote sensing technique. To fulfill this requirement, the remote sensing technique based on a microwave sensor has been developed. Since the microwave have the capability to acquire data any time and in any weather conditions with great potential (Oh et al. 2009). Microwave, due to its higher penetrating

power, can pass through the clouds, haze, or fog as well as through the crop canopy to reach the soil background beneath the crop.

The effort has been made to study the scattering mechanism of crop growth parameters for monitoring of the crop using ground-based scatterometer, airborne and space-borne SAR data (Ferrazzoli et al. 1994, Taconet et al. 1994; Han et al. 2018; Mandal et al. 2019). In these experiments, data collected at different frequencies, polarization, and incidence angles were analyzed and interpreted using various models such as the cloud model, radiative transfer and electromagnetic scattering/emission model. The ground-based scatterometer measurements were carried out at different microwave bands and full polarization (VV, HH, VH, and HV) for the selection of the optimum system and target parameters. The ground-based backscattering scatterometer have revealed high correlation between crop growth parameters such as leaf area index (LAI), biomass, and plant height (PH) with backscattering coefficients at different frequencies, polarization and angle of incidence (Attema and Ulaby 1978; Ulaby et al. 1988; Bouman 1991; Macelloni Paloscia 2001).

The study of bistatic scattering is also becoming more interesting since recent bistatic SAR mission was launched and many more are considered likely to be launched in the near future. Therefore, it is required to enhance the knowledge about the bistatic radar remote sensing techniques for accurate and timely information about crop growth monitoring. Recently, the German Aerospace Centre (DLR) and EADS Astrium launched a mission for bistatic radar system called TanDEM-X with two TerraSAR-X satellites. The TanDEM-X mission is an extension of the TerraSAR-X mission, co-flying the second satellite of nearly identical configuration (Rodriguez-Cassola et al. 2012). TanDEM-X has provided advanced expertise in the German space program, giving a significant momentum for the research and development activities, associated techniques and technologies for high resolution X-band synthetic aperture radar (SAR). The interferometric height sensitivity has doubled in bistatic

operation with respect to monostatic operation. Erten et al. (2015) investigated the capability of the TanDEM-X mission for monitoring the plant growth of the paddy-rice crop. The temporal mapping of paddy-rice crop height was compared at vertical and horizontal polarizations using TanDEM-X data. The difference in the height of the paddy-rice crop was found about 10 cm for HH- and VV-polarization data at the reproductive stage of the crop. Rossi and Erten (2015) studied the potential of TanDEM-X interferometric synthetic aperture radar images for the monitoring of biophysical parameters of the rice crop. The X-band differential bistatic interferometry radar images showed a pronounced advantage in elevation mapping of plant height of rice crop. However, the literature lacks experimental results of crops in the bistatic configuration of the radar system.

Therefore, the bistatic scatterometer measurements were conducted over the wheat crop to study the bistatic scattering mechanisms in specular direction ($\phi = 0$) at X-, C-, and L-bands for HH- and VV-polarizations in the incidence angle ranging between 10°- 60°. The specular bistatic scattering coefficient (σ^0) response of the wheat crop growth parameters was analyzed at various growth stages. The correlation analysis between σ^0 and wheat crop growth parameters were carried out to select the optimum angle of incidence, polarization and frequency for the estimation of wheat crop growth parameters using the bistatic scatterometer system. In this chapter, the estimation efficiency of the grid partition based fuzzy inference system (G-FIS) using Gaussian membership function (MF) for wheat crop growth parameters was investigated. The estimation performance of the developed G-FIS algorithm was evaluated by calculating the root mean square error (RMSE) between the observed and estimated values of wheat crop growth parameters.

4.2 EXPERIMENTAL DETAILS

An outdoor crop-bed of an area 10×10 m^2 besides the Department of Physics, IIT (BHU), Varanasi, India was prepared for bistatic scatterometer measurements at different growth stages of wheat crop. The specifications of the bistatic scatterometer system are summarized in Chapter 2. The wheat seeds of Malviya 234 (HUW-234) variety were sown in crop-bed fields at the spacing of 20 cm between the rows on 28 December 2018. The bistatic specular scatterometer measurements were carried out from 24 January 2019 to 22 April 2019 at the interval of 10 days before the wheat plants were harvested. The wheat crop growth parameters were measured simultaneously with the bistatic scatterometer measurements over the crop. The soil moisture was tried to maintain constant during the bistatic scatterometer measurement by irrigating the crop field as and when required. The average soil moisture was found gravimetrically (in %) to be 16 ±1 during the whole growth stages of the wheat crop. The detailed procedure for the measurement of crop growth parameters (FBm, LAI, PH, and VWC) of the wheat at its various growth stages is given in Chapter 2. The Equations 2.16 and 2.17 given in Chapter 2 were used for the computation of FBm and VWC, respectively.

4.3 METHODS

4.3.1 Brief description of fuzzy inference system

Fuzzy logic is an approach to computing based on "degrees of truth" rather than the usual "true or false" (1 or 0). The mapping between input and output data using fuzzy logic is called the fuzzy inference system (FIS). Membership functions (MF), logical operations, and If-Then rules are the main processing element in the fuzzy inference. In fuzzy logic, the crisp data set is converted into a data set, having the values between 0 to 1 called fuzzy set. The fuzzy inference systems are of two types based on the method of calculation of final output: Mamdani and Sugeno type. In the Mamdani type fuzzy inference system, the output is calculated by calculating the center of the area under the curve at the defuzzification step.

Whereas, in Sugeno fuzzy inference system, the output membership function is taken as a constant or linear function for each rule, and the output is calculated by taking the weighted average of all the rules (Takagi and Sugeno 1985).

For building a fuzzy inference system, the linguistic statement should be in addition to numerical data of the input and output. Then, the If-Then process is applied to characterize the relationship between the input and output fuzzy variables. For example, if there is one input x, and one output f, the two rules based on If-Then for Takagi and Sugeno model are defined as

Rule 1: If x is μ_1 Then $f_1=p_1x + r_1$

Rule 2: If x is μ_2 Then $f_2=p_2x + r_2$

Where μ_1 and μ_2 are the value of membership functions for input value x corresponding to two rules. The if-part of the rule ''x is μ_1'' is called the antecedent or premise, while the then-part of the rule ''$f_1=p_1x + r_1$'' is called the consequent or conclusion. The p_1, r_1, and p_2, r_2 are the consequent parameters of the Takagi and Sugeno inference model.

The fuzzy inference system consists of five steps such as: to fuzzify the input, to apply the fuzzy operator (AND or OR) in the antecedent, to implicate the antecedent by using the above mentioned processing element in fuzzy inference, aggregate all the consequent through the rules and defuzzify the aggregate output to find the final output value (Zadeh 1965; Tagaki and Sugeno 1985).

3.2 Grid partition based fuzzy inference system (G -FIS)

In this method, the input data is partitioned into regions that are predefined by membership function using axis parallel partition called the grid. These grids are then used to generate fuzzy rules based on system input-output data (Abonyi et al. 1999).

For mapping the one input variable and one output variables using the grid partition based fuzzy inference system, the input data is partition into the different number of grids according to the following equations as (Chung et al. 2007).

$$m_i^K = x_{min} + (x_{max} - x_{min}).\frac{i-1}{K-1} \quad (4.1)$$

$$n^K = \frac{(x_{max}-x_{min})}{K-1} \quad (4.2)$$

Where K is the number of the partition (number of membership function), i=1, 2, 3…K, m_i^K is the center point of the membership function, n^K is the distance from the center point to the endpoint of the membership function and x_{max} and x_{min} denote the maximum and minimum values of the input data, respectively.

Now, by partitioning the input data into a different number of grids, the input and output data will automatically be mapped according to the number of grids as

R_i^k: If x is μ_i^k Then $f_i = p_i x + r_i$, where. i=*1, 2, 3....K*

Then, the final output is calculated as

$$f = \frac{\sum_{i=1}^{k} \mu_i^k f_i}{\sum_{i=1}^{k} \mu_i^k} \quad (4.3)$$

In the present study, the ***genfis1*** function of the fuzzy logic toolbox in MATLAB was used for the estimation of wheat crop growth parameters.

4.4 RESULTS AND DISCUSSION

Figure 4.1 shows the temporal variation of wheat crop growth parameters during the entire growth cycle. All the crop growth parameters were found to be increasing trend with the age of crop, reached to a maximum value on 88 days after sowing except LAI and then they started to decline afterward. The LAI reached to a maximum on 78 days after sowing and then declined afterward. Figures 4.2-4.7 show the temporal variation of bistatic specular scattering coefficient ($\sigma°$) of wheat crop at different incidence angle ranging from 20°- 60° at

a step of 10° at X-, C-, and L-band for HH- and VV-polarizations. The values of $\sigma°$ were found decreasing trend with the age of crop for both the polarizations and reached to minimum on 88 days and then started to increase for all the X-, C- and L- bands at both the polarizations. The decreasing trend of $\sigma°$ for all the three bands at both the polarizations are attributed to attenuation and reduction in reflected components of the incident microwave from the soil background beneath the crop in the specular direction. At older stages i.e. after the maturity stage of the wheat crop, the crop growth parameters started to decrease; therefore, the attenuation caused to the coherent contribution of the incident radiation by the crop (lower plant height and vegetation water content) in the specular direction was low in comparison to the earlier growth stages. Therefore, the coherent component of the incident radiation by the soil background beneath the crop started to increase again; hence the value of $\sigma°$ was found to enhance after 88 days from the date of sowing. The values of C-band $\sigma°$ were found to be higher than X-band at the early three growth stages of the wheat crop. However, at the later growth stage of the crop, the highest values of $\sigma°$ were found at X-band. The highest value of $\sigma°$ at C-band is attributed to both the strongest direct crop canopy scattering and scattering from the soil background beneath the crop at the early growth stage of the crop. While at the later growth stage, at C-band, only crop canopy scattering was found strong, and soil background beneath the crop scattering was low due to the higher attenuation in crop canopy caused by increased slant path of the incident microwave radiation into the crop canopy. Therefore, there was a significant decrease in the scattering components due to soil background, and only crop canopy scattering was found to be the dominant scattering components at C-band frequency. Therefore, the highest value of $\sigma°$ was found at X-band at later growth stage of the crop because of the strongest direct crop canopy scattering at higher frequencies. The lowest value of $\sigma°$ was attributed to dominant volume scattering from the soil ground beneath the crop for L-band frequency, and hence, the attenuation caused by

higher penetration into crop canopy for longer wavelengths was highest than X- and C-bands (Liang et al. 2005). In addition, the HH-polarization $\sigma°$ was found higher than VV-polarization. Since vertical stalks of the wheat crop are modeled as vertically oriented lossy dielectric cylinder. Therefore, there was more interaction of VV-polarizations with the vertical stalks of the wheat crop for all the three bands causing to lower value of $\sigma°$ at VV-polarization as compared to HH-polarization.

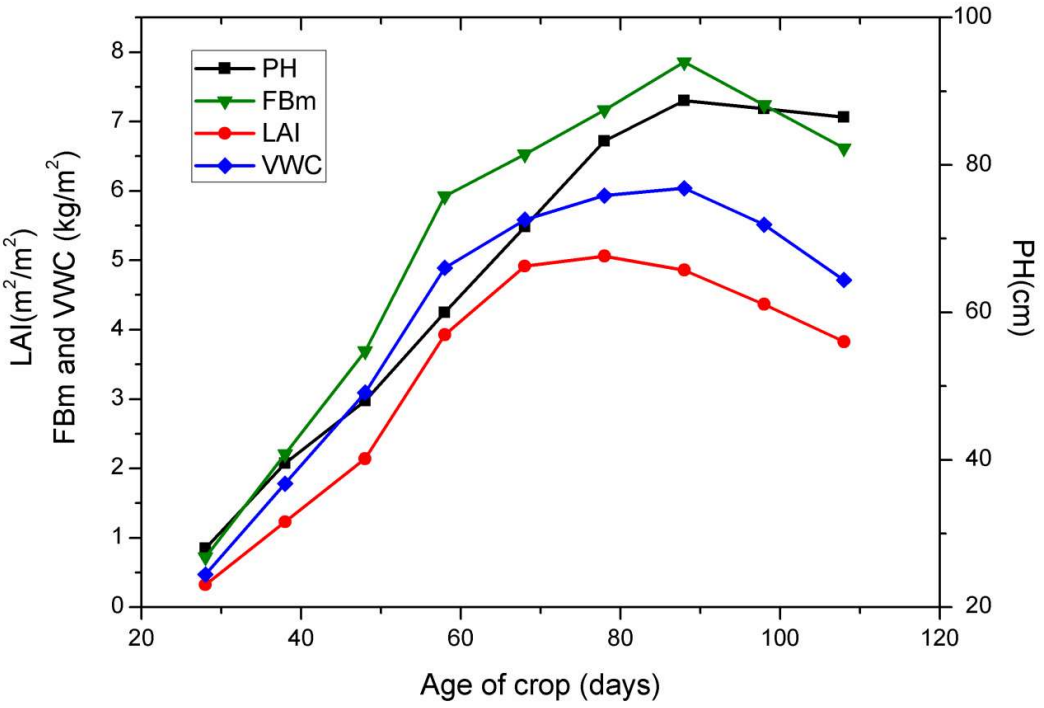

Figure 4.1 Temporal variation of wheat crop growth parameters

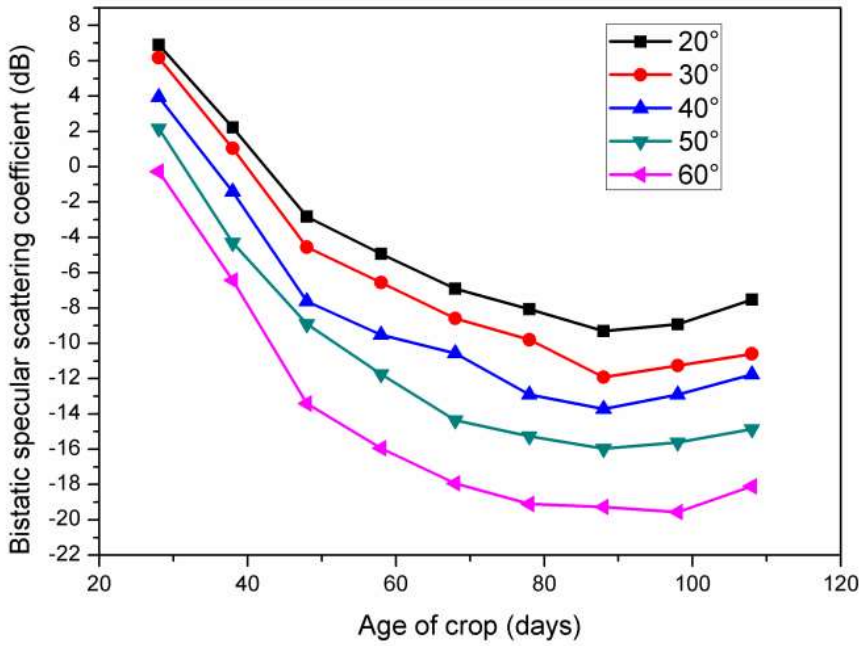

Figure 4.2 Temporal variation of σ° at X-bands for HH-polarization

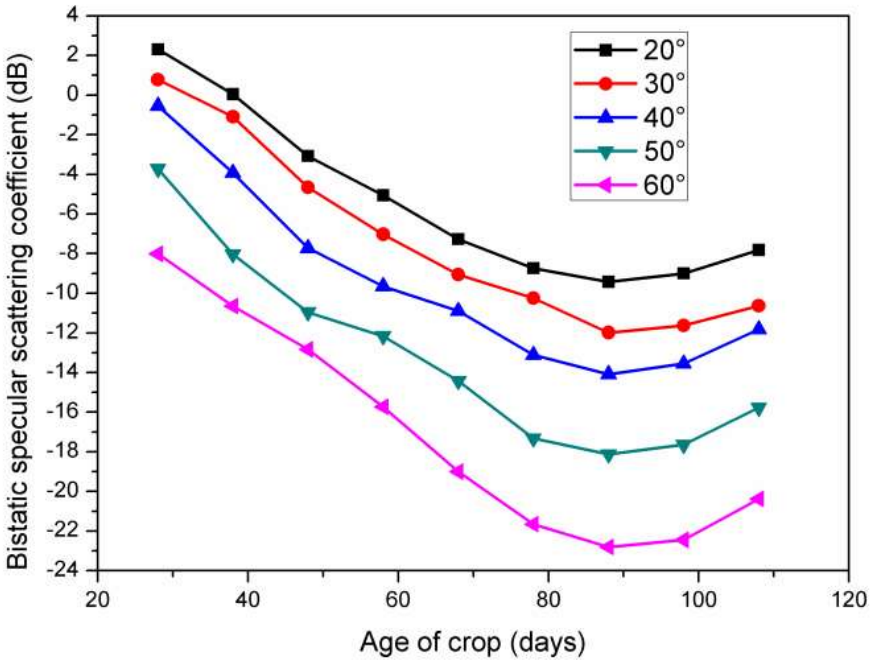

Figure 4.3 Temporal variation of σ° at X-bands for VV-polarization

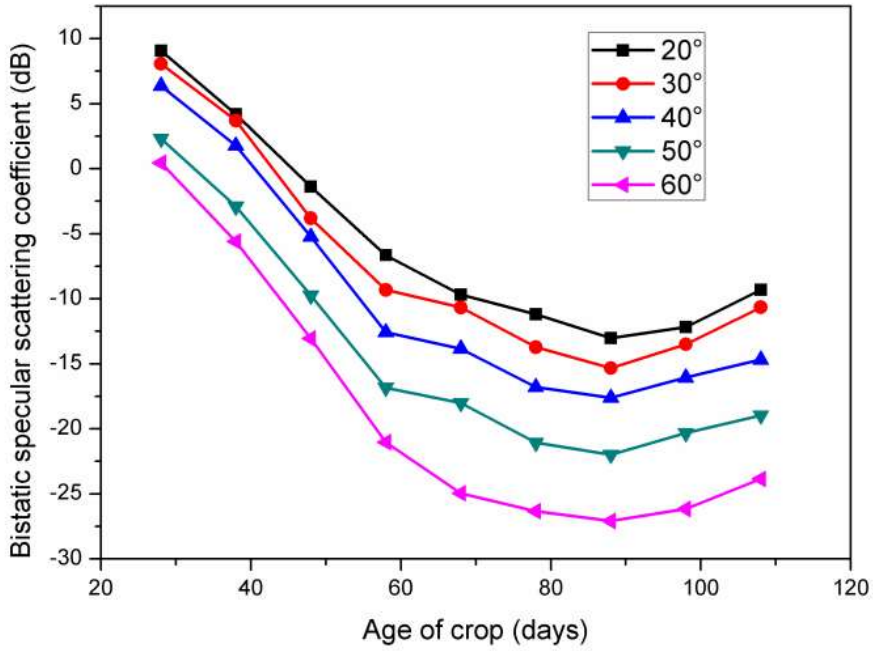

Figure 4.4 Temporal variation of σ° at C-bands for HH-polarization

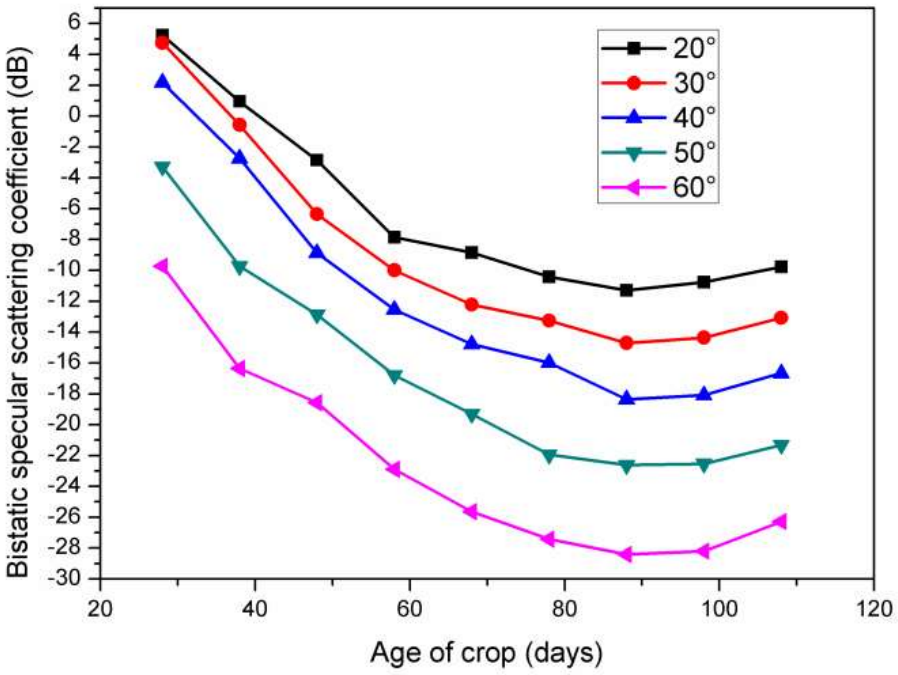

Figure 4.5 Temporal variation of σ° at C-bands VV-polarization

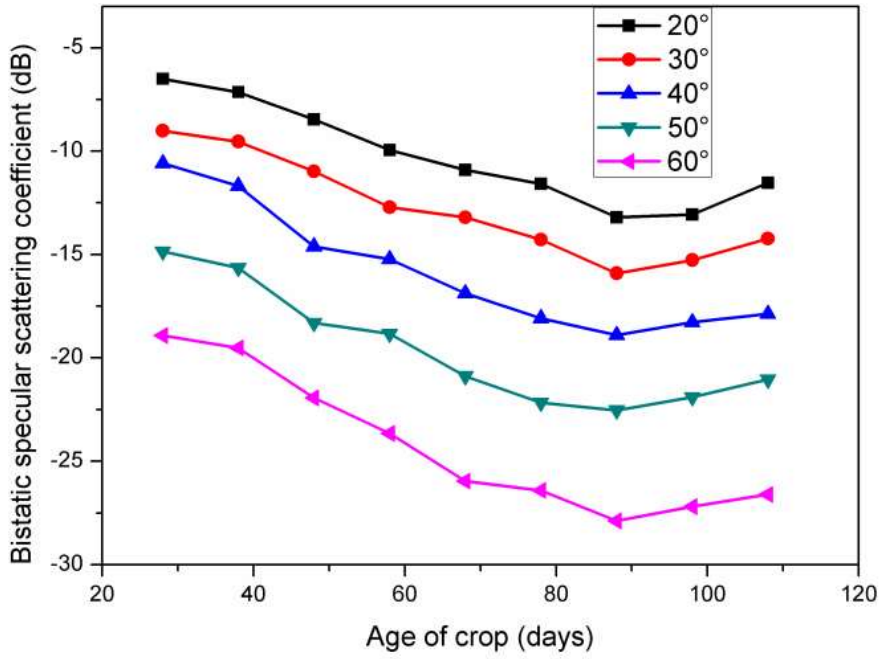

Figure 4.6 Temporal variation of σ° at L-bands for HH-polarization

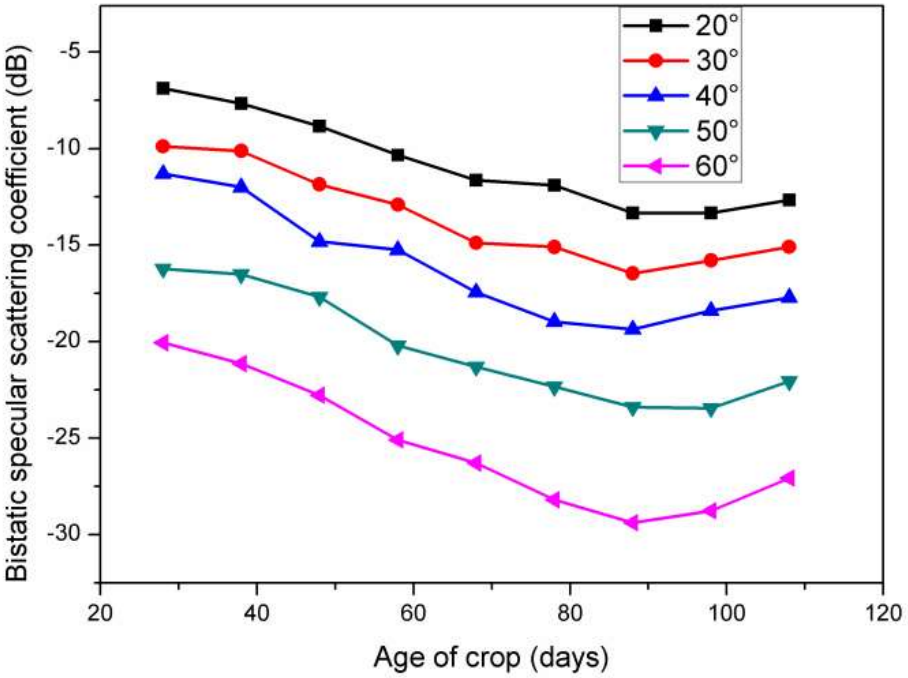

Figure 4.7 Temporal variation of σ° at L-bands for VV-polarization

The values of σ° for each band and polarization have different angular dynamic ranges from 20° to 60°. The dynamic range at the older stage crop was found greater as compared to the early growth stage of the crop for each band and polarization. Since, at the early growth stage, the soil background beneath the crop scattering components is dominant (due to smaller values of crop growth parameters) for all the angle of incidence. At the later growth stage of the crop, the soil background beneath the crop scattering component is low due to higher attenuation by crop (due to larger values of crop growth parameters). This attenuation is more at a higher angle of incidence (due to higher slant path) as compared to the lower angle of incidence at later growth stage of the crop leading to the higher dynamic range of σ° with the growth stages of wheat crop. Thus, values of the angular dynamic range of σ° for each band and polarization showed very distinct behaviours at different growth stages, which can be used to discriminate the early and later growth stages of the wheat crop.

Table 4.1 Coefficient of determination (R^2) between the bistatic specular scattering coefficient and wheat crop growth parameters for X- and C-band at 40° incidence angle and for L-band at 50° incidence angle for HH- and VV-polarization

Crop growth parameters	Coefficient of determination (R^2)					
	X-band		C-band		L-band	
	HH-pol	VV-pol	HH-pol	VV-pol	HH-pol	VV-pol
FBm	0.956	0.978	0.982	0.978	0.954	0.943
LAI	0.891	0.908	0.954	0.902	0.904	0.869
PH	0.884	0.939	0.966	0.941	0.952	0.956
VWC	0.943	0.951	0.978	0.943	0.925	0.882

The optimum angle of incidence, polarization, and frequency of the bistatic scatterometer system was found by analyzing the correlation between the wheat crop growth parameters and $\sigma°$ for the estimation of crop growth parameters by grid partition based fuzzy inference system (G-FIS) using Gaussian membership function (MF). Correlation analysis showed that high coefficient of determination (R^2) was found at 40° incidence angle for X- and C-bands whereas at 50° incidence angle for L-bands. However, Table 4.1 shows that R^2 was found higher at VV-polarization for X-band and at HH-polarization for C - and L-bands. The results of the correlation analyses also showed that C-band for HH-polarization had the highest R^2 with all the crop growth parameters.

Based on the observed high correlation between σ^0 at three bands for both the polarizations and crop growth parameters, G-FIS algorithm was developed for the estimation of crop growth parameters using σ^0 data at 40° incidence angle for HH-polarization at C-band. Root mean square error (RMSE) was used as a metric for assessing the estimation performance of the developed G-FIS algorithm. Now, the interpolations of the data from 28 to 108 days into 81 days data sets at the interval of one day were done to find the additional data sets for the training and testing of the G-FIS algorithm. From this 81 data set, 61 data was used for the training the G-FIS, and every fourth data at the interval of 3 days were taken for testing the G-FIS. The G-FIS algorithm was developed by taking the values of σ^0 as input data and crop growth parameters FBm, LAI, PH and VWC as output data for training.

The optimum number of Gaussian MF for G-FIS algorithm should be chosen for generating the number of fuzzy rules between the input and output data sets. Since, larger number of Gaussian MF will result larger number of fuzzy rules leading to over fitting the training and testing data while the smaller number of Gaussian MF generates smaller number of fuzzy rules leading to courser model. Therefore, optimum number of Gaussian MF for G-FIS algorithm should be chosen for the good balance between the number of fuzzy rules and

RMSE values due to larger number of Gaussian MF for the partition of the input data sets. In the case of G-FIS model setting, the optimum number of MF (Gaussian) for partitioning the input data was chosen in order to have good balance between the number of fuzzy rules and RMSE for the estimation of crop growth parameters. The optimum number of MF was chosen by training the algorithm using different number of MF from 2 at the steps of 1 by trial-error method and calculating the RMSE values between observed and estimated values at different number of MF (Abonyi et al. 1999). The optimum number of MF and hence the optimal model was chosen where RMSE values for the training and testing data started to diverge.

Table 4.2 The optimum values of various parameters of G-FIS algorithm at C-band for HH-polarization

Crop growth parameters	FBm	LAI	PH	VWC
Optimum number for grid partition	5	5	5	5
Number of fuzzy rules	5	5	5	5
Number of membership functions	5	5	5	5
RMSE (training)	0.0687	0.1183	1.6287	0.1084
RMSE (testing)	0.0775	0.1334	1.9387	0.1304

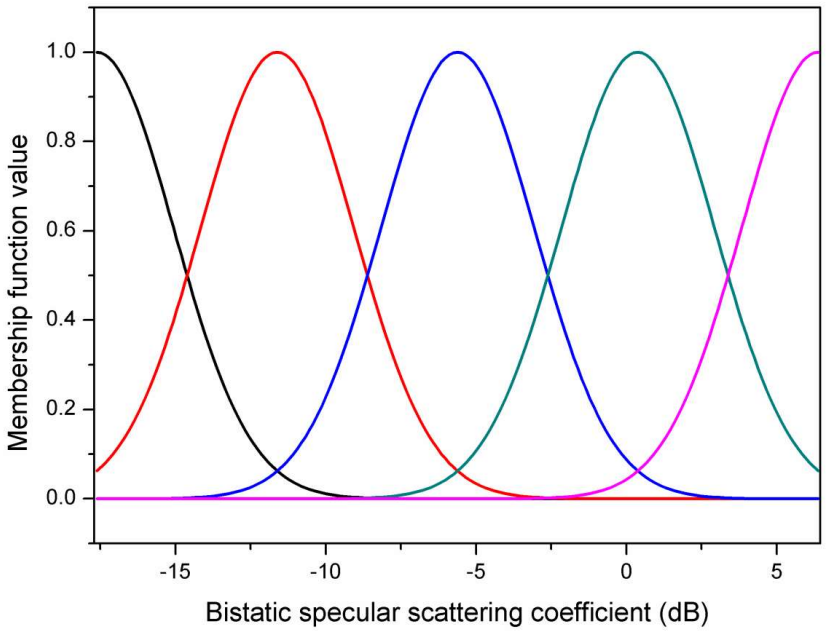

Figure 4.8 Membership function plot for HH-polarization at C-band

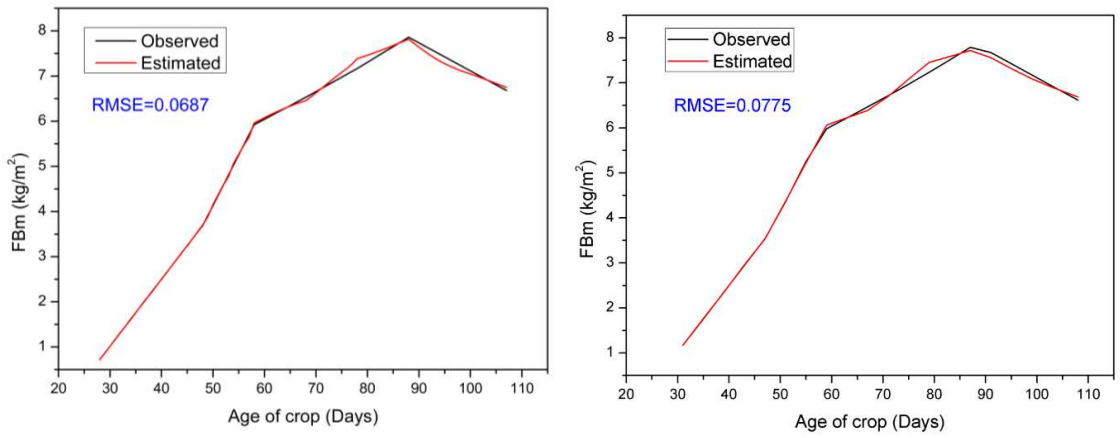

(a) **(b)**

Figure 4.9 Fuzzy algorithm performance for the estimation of FBm at 40° angle of incidence for HH-polarization at C-band for (a) training and (b) testing

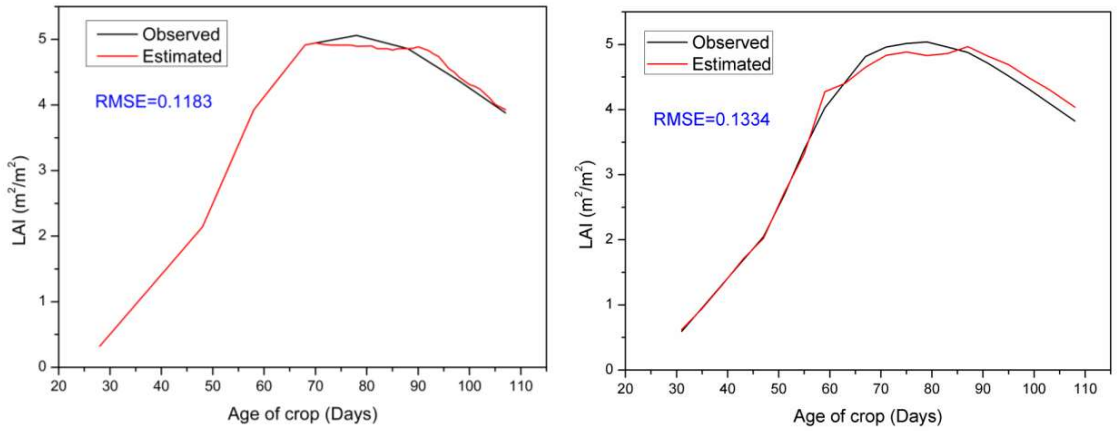

(a) **(b)**

Figure 4.10 Fuzzy algorithm performance for the estimation of LAI at 40° angle of incidence for HH-polarization at C-band for (a) training and (b) testing

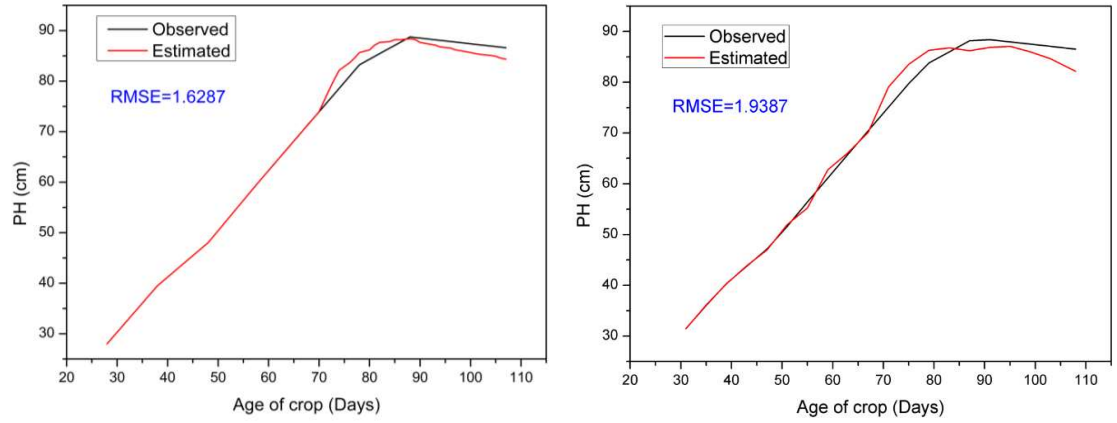

(a) **(b)**

Figure 4.11 Fuzzy algorithm performance for the estimation of PH at 40° angle of incidence for HH-polarization at C-band for (a) training and (b) testing

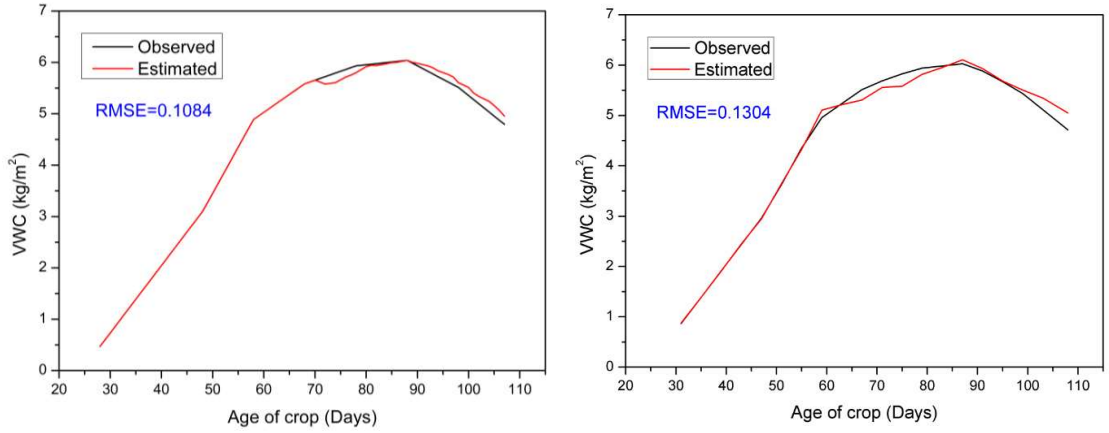

(a) **(b)**

Figure 4.12 Fuzzy algorithm performance for the estimation of VWC at 40° angle of incidence for HH-polarization at C-band for (a) training and (b) testing

Tables 4.2 summarizes RMSE values between the estimated and observed crop growth parameters for the optimized number of MF and various other parameters of the G-FIS algorithm. The optimum number of MF was found to be 5 for the estimation of crop growth parameters. Table 4.2 shows the lowest RMSE for the estimation of FBm followed by VWC, LAI, and PH. Therefore, the performance of the developed G-FIS algorithm is considered to be very good for all the crop growth parameters at C-bands for HH-polarization. Figure 4.8 shows the MF curve for different crop growth parameters at C-band for HH-polarization. The performance of the developed G-FIS algorithm is also represented by temporal variation of the estimated and observed crop growth parameters for the training and testing data as shown in Figure 4.9-4.12. However, the estimation of crop growth parameters requires an understanding of the scattering mechanism of microwave radiation with the crops scattering elements, exact expressions between σ^0 and crop growth parameters and accurate numerical values of the measured crop growth parameters. Nevertheless, due to the learning capability of the fuzzy inference system from the input and output data space

only, it can be used to estimate the parameters of a physical system involving the complex mathematical expression.

5.5 CONCLUSIONS

The bistatic scattering coefficients ($\sigma°$) were found to decrease with the increase in crop growth parameters. The high values of coefficient of determination (R^2) were found at 40° incidence angle for VV- and HH-polarizations at X-band and C-band, respectively. Whereas, the correlation coefficient was found high at 50° incidence angle for HH-polarization at L-band. At the early growth stages of the wheat crop, both the crop canopy and soil background beneath the crop scattering were found to be dominant scattering components at C-band. The performance index RMSE showed that the estimated values of crop growth parameters by the developed G-FIS algorithm based on Gaussian MF were found very close to the observed values. The estimated values of wheat crop growth parameters by the developed algorithm were found better for FBm as compared to other crop growth parameters at C-band for HH-polarization. Therefore, these results may be suggested for the future bistatic radar system to monitor the wheat crop fields.